J Bionic Eng 18 (2021) 786–798
DOI: https://doi.org/10.1007/s42235-021-0058-3
Journal of Bionic Engineering
http://www.springer.com/journal/42235

Stable Vertical Ladder Climbing with Rung Recognition for a Four-limbed Robot

Xiao Sun[1*], Kenji Hashimoto[2], Shota Hayashi[3], Masahiro Okawara[3], Takashi Mastuzawa[3], Atsuo Takanishi[3]

1. *Department of Mechatronics*, *University of Yamanashi*, *Yamanashi* 400-8511, *Japan*
2. *Department of Mechanical Engineering Informatics*, *Meiji University*, *Tokyo* 214-8571, *Japan*
3. *Faculty of Science and Engineering*, *Waseda University*, *Tokyo* 162-8480, *Japan*

Abstract

This paper proposes a system for stable ladder climbing of the human-sized four-limbed robot “WAREC-1”, including the following 3 components: (a) Whole-body motion planning; (b) Rung recognition system and (c) Reaction force adjustment. These 3 components guarantee appropriate ladder climbing motion, successful rung grub and proper reaction force distribution at contact points throughout the climbing motion, respectively. With this system, (1) Stable ladder climbing in 2-point contact gait by a human-sized robot and (2) Successful and stable climbing of an irregular ladder (with a higher or inclined rung) in both 3-point and 2-point contact gait with the capability of recognizing the target rung and the corresponding motion planning are realized, which have rarely been realized by former studies. Finally, experiment results and data of the robot ladder climbing are also presented to evaluate the proposed system.

Keywords: legged robot, ladder climbing, stability, proximity sensor feedback, force control

1 Introduction

The locomotion of robots as the substitute of human has always been a hot topic in research of robotics, but as a locomotion style ladder climbing performed by robots has not been as concerned as other popular types of locomotion, such as multi-legged walking or flying. However, it is also the truth that as a type of common tool for vertical locomotion, ladders are very popular in both indoor and outdoor situations. They are relatively cheap, easy to be manufactured and attached to walls and require the less space in comparison with other means of vertical locomotion, such as stairs and elevators. In this paper, the authors focus on ladder climbing by human-sized four-limbed robots besides other types of locomotion styles. The aim is developing a robot platform with the versatility of locomotion and manipulation and finally putting it into practical use, such as disaster response and maintenance of infrastructures as well as aged plants. Details can be seen in the former papers of the author(s)[1,2].

The history of vertical ladder climbing by robots is relatively short compared with other locomotion styles. In 1989, LCR-1, the first robot ladder climber was developed[3]. After that, solutions of Gorilla-III (child-sized)[4–7], Atlas (with an inclined ladder instead of vertical ones)[8], HRP-2[9,10] and E2-DR[11,12] (human-sized) were developed. As for robot ladder climbers with smaller sizes, hexapod robot ASTERISK[13], Felidae-like robot[14] developed by Tokyo Metropolitan University and the lightweight (2.2 kg) ladder climbing robot with 4 hooks lined up in a row[15] are representative instances. Besides legged robot with end-effectors, snake robot also emerged as another robotic solution of vertical ladder climbing[16,17]. Among various solutions of ladder climbing for robots in different sizes, in consideration of enhancing locomotion and manipulation capability in environment designed for human, this paper mainly focuses on vertical ladder climbing of human-sized robots.

In former related studies of Refs. [18–21], although motion generation of ladder climbing is systematically studied, the discussion of stability in ladder climbing has still been mainly based on conventional and general theories used on legged walking. However, stability considering the recognition of ladder rung as well as the

***Corresponding author:** Xiao Sun
E-mail: xsun@yamanashi.ac.jp

corresponding motion generation for climbing is rarely discussed, neither is its application to the real robots. Although Yoneda *et al*. proposed a recovery motion model for Gorilla-III in the case of grip fail of rungs[4], the judgment of success/failure of grip was done by the output of voltage from end-effectors, which is only conditionally effective for failed grip of the target rung but could not deal with inappropriate grip of the rungs and quantitative correction of motion planning. For recent studies, Ref. [22] proposed a ladder detection system with Kinect as the sensor and detection by the processing of obtained point cloud data with the algorithm of RANSAC and others, which is verified in the simulation with ladder climbing motion of the robot PR2. As for the ones with real robots, E2-DR is claimed to be capable of recognizing a ladder by point cloud data acquired from LRFs (Laser Range Finder) with "relatively high precision"[6]. Yet it requires proper calibration of sensors, which may be difficult in application, and there are no quantitative data or experimental verification provided about the precision of recognition as well as its relationship with stability. Study of Ref. [15] also claimed that rung recognition is applied in ladder climbing with ultrasonic sensors, but unfortunately there is no details about its sensing or its verification and evaluation about accuracy. In addition, the target ladders in the former studies are all normal ladders. However, in practical use of ladder climbing by robots there is no guarantee that the specification of the target ladder can be obtained in advance, let along with the case that the ladder is damaged and deformed due to aging or other reasons.

Therefore, this paper proposes a solution that enables stable ladder climbing based on recognition of ladder rung to climb, with the sensor feedback of both proximity sensors for rung recognition and force/torque sensors for maintaining stability during climbing. As a result, a system integrating whole-body motion planning, reaction force feedback control for stability and rung recognition without mutual conflict is proposed. Afterwards, evaluation experiments about climbing an irregular ladder are also presented.

This paper is organized as follows: Section **2** briefly introduces the robot hardware (especially for end-effector) related to ladder climbing as the prerequisite knowledge. Section **3** describes the whole stabilization system of ladder climbing for WAREC-1, including (i) The scheme of whole-body motion planning for ladder climbing of WAREC-1 and the stability condition that it is based on; (ii) Rung recognition system for ladder climbing of WAREC-1 and (iii) Reaction force adjustment, an indispensable method for stable ladder climbing when there are only 2 contact points between the robot and ladder. Section **4** demonstrates evaluation experiments of WAREC-1, integrating all contents explained in this paper with results, data and discussions of the experiments presented, which are also main contribution of this paper along with section **3**. Finally, section **5** summarizes this paper and prospective works to be done.

2 Robot hardware related to ladder climbing

WAREC-1 (WAseda REsCuer-No.1) is the human-sized four-limbed robot developed by Takanishi Laboratory, Waseda University, Japan. Its specification, design concepts and locomotion performance in different styles are introduced and described in the former paper of the authors[1]. Its overview, scale and configuration of Degree of Freedom (DoF) are shown in Fig. 1.

With the aim of being a robot platform of disaster response as well as inspection of infrastructure and plants, so far WAREC-1 has realized locomotion styles including but not limited to vertical ladder climbing[23,24], biped/quadruped walking, stair climbing, wheel driving and crawling[25], a locomotion style that the body and limbs of robot contact the ground by turns. With the versatility of locomotion styles described above, the accessibility and adaptability of WAREC-1 in

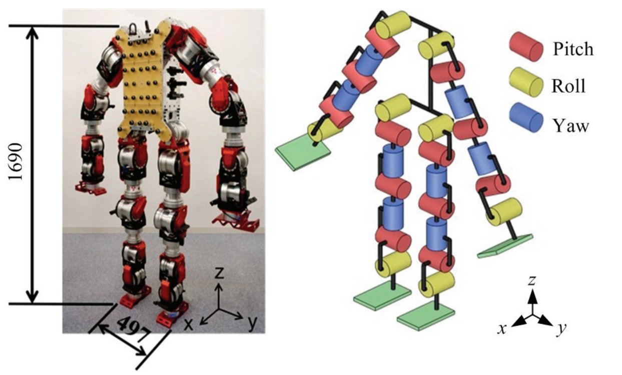

Fig. 1 Overview and DoF configuration of WAREC-1.

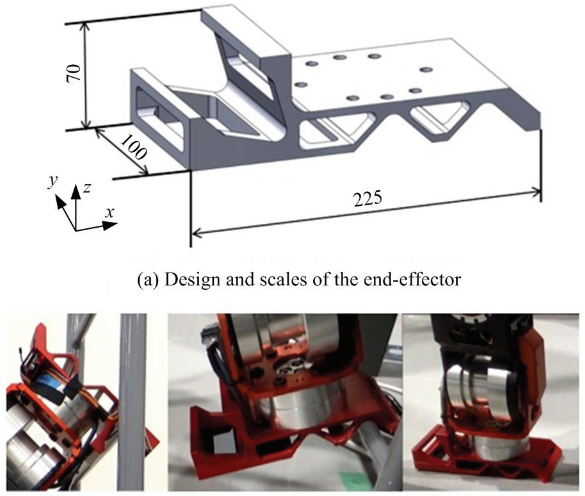

(a) Design and scales of the end-effector

(b) As a hand in ladder climbing (c) As a foot in ladder climbing (d) Surface contact in legged stance

Fig. 2 End-effector of WAREC-1.

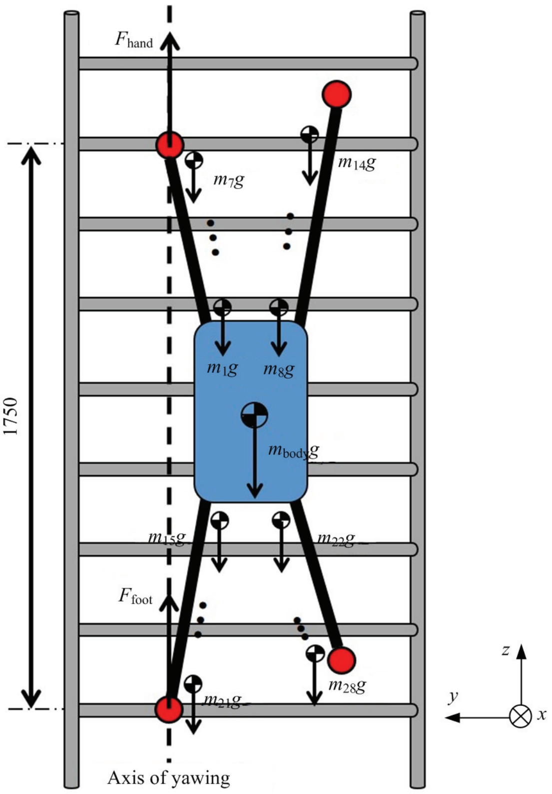

Fig. 3 Illustration of WAREC-1 on a ladder.

complicated environment are strongly supported. All 4 limbs of WAREC-1 have identical structure and design so that the robot has symmetry in both up-down and left-right direction. This feature guarantees the compatibility of all limbs and robustness for the case that one limb of WAREC-1 is broken or out of control. Similarly, end-effectors of WAREC-1 also share the same design that can be used for both hand and foot in ladder climbing and realize surface contact for legged stance like Fig. 2. The detailed design of the end-effector can be seen in Ref. [26].

As for sensors, there is a force/torque sensor equipped at each end-effector (4 in total), an IMU (Inertial Measurement Unit) inside the body of robot and 2 proximity sensors at each end-effector (8 in total).

3 Stabilization system of WAREC-1

3.1 Whole-body motion planning with stability condition of ladder climbing

The motion generation for WAREC-1 has been detailly introduced and described in the previously published works of the authors[2,23,24]. Here, brief explanation of ideas and schemes proposed by the authors about ladder climbing motion planning of WAREC-1 will be given as a reference.

3.1.1 Stability conditions for motion planning

Different from other types of legged locomotion styles, stability in ladder climbing has the highest priority, because it is extremely difficult for a robot to recover after falling from a ladder, with much bigger impact force exerted to the robot.

Since stability must always be guaranteed throughout ladder climbing motion, the description of stability analysis goes first before the detailed discussion. Former study of Gorilla-III[4] has presented that there should be no rotation around AoY (Axis of Yawing) and contact points for stable ladder climbing motion, and our study expanded its idea from single-mass static model to multi-mass model dynamic model[24] with illustration in Fig. 3. The stability conditions of WAREC-1 can be given as:

$$\sum \boldsymbol{M} = \boldsymbol{M}_{\mathrm{g}} + \boldsymbol{M}_{\mathrm{ext}} = 0, \tag{1}$$

$$\sum \boldsymbol{M}_{\mathrm{AoY}} = \boldsymbol{R}_{\theta}\left(\boldsymbol{M}_{\mathrm{g}} + \boldsymbol{M}_{\mathrm{ext}}\right) = 0, \tag{2}$$

where

$$\boldsymbol{M}_{\mathrm{g}} = \sum_{i} (\boldsymbol{r}_i \times m_i \boldsymbol{g}), \tag{3}$$

$$\boldsymbol{M}_{\mathrm{ext}} = \boldsymbol{M}_{\mathrm{hand}} + \boldsymbol{M}_{\mathrm{foot}}, \tag{4}$$

$$\boldsymbol{M}_{\text{hand}} = \boldsymbol{r}_{\text{hand}} \times \boldsymbol{F}_{\text{hand}}, \tag{5}$$

$$\boldsymbol{M}_{\text{foot}} = \boldsymbol{r}_{\text{foot}} \times \boldsymbol{F}_{\text{foot}}, \tag{6}$$

where $\sum \boldsymbol{M}$ is the total sum of moment around the origin, $\sum \boldsymbol{M}_{\text{AoY}}$ is the total sum of moment around AoY[4], $\boldsymbol{M}_{\text{g}}$ is the total sum of gravity moment, $\boldsymbol{M}_{\text{ext}}$ is the total sum of external force (force at contact points between the robot and ladder) moment, θ is the inclination angle of AoY around x-axis in Roll, $\boldsymbol{R}_\theta$ is the 3-Dimensional rotation matrix with rotation of θ in Roll, i is the number of the link in the robot (the body of robot is also included), $\boldsymbol{r}_i$ is the displacement vector from the origin to CoM of the i_{th} link, m_i is the mass of the i_{th} link, $\boldsymbol{g}$ is the acceleration of gravity, $\boldsymbol{M}_{\text{hand}}$ is the moment of force at the supporting hand, $\boldsymbol{M}_{\text{foot}}$ is the moment of force at the supporting foot, $\boldsymbol{r}_{\text{hand}}$ is the displacement vector from the origin to the contact point on hand, $\boldsymbol{r}_{\text{foot}}$ is the displacement vector from the origin to the contact point on foot, $\boldsymbol{F}_{\text{hand}}$ is the force at the supporting hand, and $\boldsymbol{F}_{\text{foot}}$ is the force at the supporting foot. The origin is defined as the contact point of foot. If both 2 feet are in contact with the ladder, then the one on left foot will be the origin. Eq. (1) and Eq. (2) express the equilibrium of moment around the origin and AoY, respectively. They can be written as

$$\sum \boldsymbol{M} = \sum_i (\boldsymbol{r}_i \times m_i \boldsymbol{g}) + \boldsymbol{r}_{\text{hand}} \times \boldsymbol{F}_{\text{hand}} + \boldsymbol{r}_{\text{foot}} \times \boldsymbol{F}_{\text{foot}} = 0, \tag{7}$$

$$\sum \boldsymbol{M}_{\text{AoY}} = \boldsymbol{R}_\theta \left(\sum_i (\boldsymbol{r}_i \times m_i \boldsymbol{g}) + \boldsymbol{r}_{\text{hand}} \times \boldsymbol{F}_{\text{hand}} + \boldsymbol{r}_{\text{foot}} \times \boldsymbol{F}_{\text{foot}} \right) = 0. \tag{8}$$

Since Eq. (8) is always satisfied if Eq. (7) is satisfied, then stable ladder climbing must at least satisfy Eq. (7), which means that stability condition Eq. (1) and Eq. (2) can be simplified as Eq. (7).

3.1.2 Scheme of whole-body motion planning

The whole-body motion planning of ladder climbing for WAREC-1 can be mainly divided into the following 3 parts: (i) Ladder climbing gaits; (ii) End-effector trajectory and (iii) Body trajectory. In our study, climbing gaits will be chosen first according to different situations (by judge of human so far), then whole-body motion for ladder climbing can be planned with the combination of end-effector trajectory and body trajectory, consideration of stability condition Eq. (7).

3.1.3 Ladder climbing gaits

For simplicity and comprehensibility, this paper describes the order and number of limbs to move in ladder climbing as quadruped walking gaits, which is popular in related studies[4–12]. For ladder climbing, major gaits can be divided into 3-point contact gait and 2-point contact gait. While in 3-point contact gait 4 limbs move one by another so that there are always at least 3 contact points, in 2-point contact gait 2 limbs moves simultaneously for climbing. Apparently, it takes fewer steps for 2-point contact gaits to climb up/down a rung, but it also has much higher risk of rotation around contact points or AoY axis connecting them, which may cause the failure of ladder climbing. Actual moves of these 2 gaits can be seen in the section **4**.

From different features of these 2 types of ladder climbing gaits, it can be concluded that 3-point contact gait is better for cases where there is no requirement about the climbing speed, while 2-point contact gait may be chosen for cases that 3-point contact gait is too slow to meet the requirement and stability can be somehow guaranteed. In this paper, both 2 types of gait are discussed.

3.1.4 End-effector trajectory planning

For WAREC-1, path-time independent end-effector trajectory planning with path length optimization (always choose the shortest path length possible) has been proposed by the authors so that path and time profile of the end-effector can be planned individually to meet respective needs or constraints. Arc-length parameterization is utilized for separating path and time in end-effector trajectory. More details can be seen in the former work of the authors[23].

3.1.5 Body trajectory planning

In our study, the body trajectory of ladder climbing is determined by gaits with consideration of stability condition Eq. (7). Specifically, for 3-point contact gait there will be only vertical movement for the body, with the length of 1/4 of the rung interval for each step so that 4 steps in 3-point contact gait is cyclic. For 2-point contact gait, horizontal movement of body will be added for stability. The distance of horizontal move of body is determined by both stability conditions and the reachable range of WAREC-1 to make sure that the climbing motion in 2-point contact gait is both feasible and stable, or at least as close to stable state as possible[24]. Specific robot motion can be seen in section **4**.

3.2 Rung recognition in ladder climbing

3.2.1 Proximity sensor system

In this subsection, efforts in realizing stable ladder climbing in terms of guaranteeing appropriate contact between the robot and ladder are mainly described. As is introduced in section **2**, hook-shaped structure and 2 grooves on end-effectors of WAREC-1 in Fig. 2 contribute to stable grub of rungs and avoid slip in ladder climbing in comparison with flat end-effectors, which are commonly used for the former ladder climbing robots, especially for foot[4–12]. In addition, they also enable position error absorption to a certain degree, depending on the relationship between the diameter of ladder rungs to climb and the width of them.

Furthermore, combined with the design of end-effector, proximity sensor system has also been applied to error compensation for both position and orientation in ladder climbing[27,28]. The summary of proximity sensor system about the sensor, position of sensors equipped at the end-effectors and the whole proximity sensor system configuration are depicted in Fig. 4. Error compensation by this sensor system is indispensable for ladder climbing of WAREC-1 because its long limbs (about 1.1 m) and heavy weight (155 kg) may cause deformation that is too big to be absorbed by the end-effector, depending on the posture of WAREC-1.

With the efforts above, success rate of rung grub for climbing a normal ladder with known rung interval has improved greatly. Nevertheless, ladder climbing in real application needs to go further because (i) Specification of ladders in application differs from each other and it may be difficult to obtain specification data in advance and (ii) Ladders in reality may be deformed or even damaged (rusted, broken, *etc.*). Unfortunately, few human-sized robots have been claimed to be capable of dealing with these two issues, and this paper gives a partial solution as well as experimental verification with utilization of the proximity sensors system.

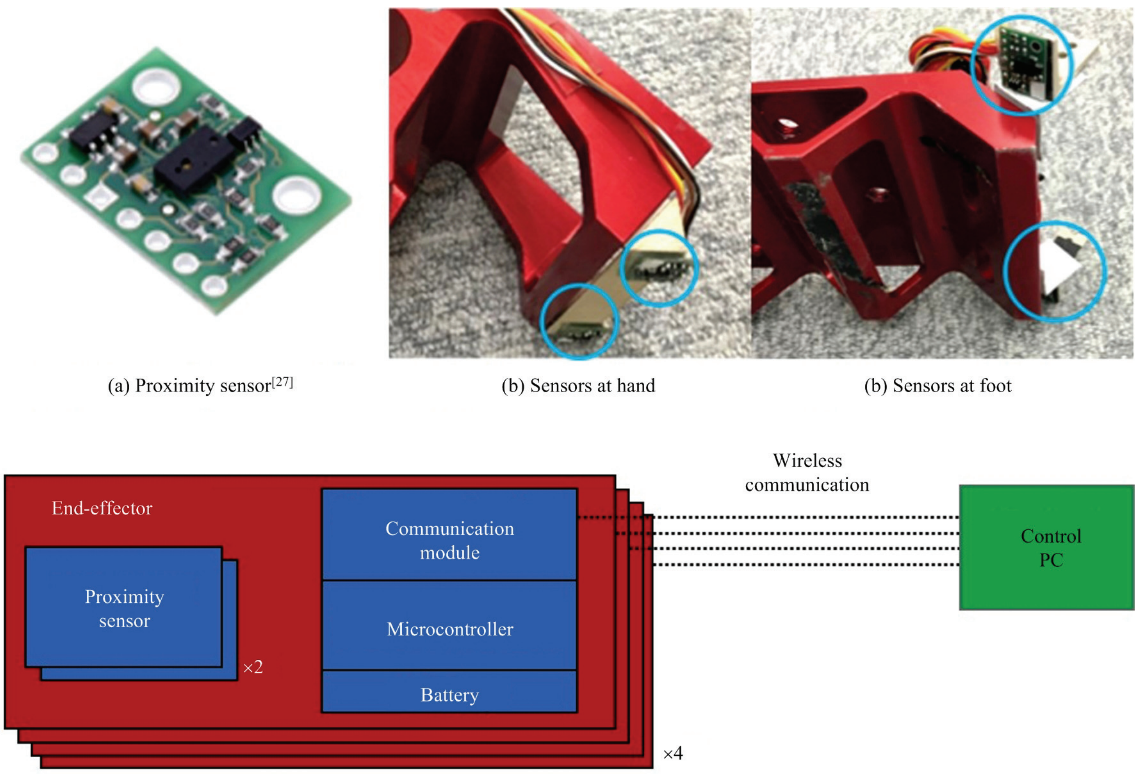

(a) Proximity sensor[27] (b) Sensors at hand (b) Sensors at foot

(d) System configuration

Fig. 4 Summary of proximity sensor system.

3.2.2 Mechanism of rung recognition

As is described in Ref. [28], proximity sensor system for WAREC-1 measures not only the relative position (in x and z-axis) but also orientation (in Roll and Yaw) between the robot and target ladder rung. That is the reason why there are 2 proximity sensors for each end-effector instead of only one. Although proximity sensors chosen satisfy the accuracy required for ladder climbing (less than 5 mm) and is sufficiently small to be equipped on end-effectors directly, it also has the drawback of short measurable range and narrow FoV (Field of View) as the expense, which makes it difficult for WAREC-1 to recognize ladder rungs without moving.

Consequently, for the recognition of ladder rungs to climb, sensing approach called "scan motion" is applied and integrated with climbing motion of the end-effector. As its name, this motion moves the end-effector forward along x-axis until 2 proximity sensors both pass over the target rung. As Figs. 4b and 4c show, the attaching angles of proximity sensors are fixed, thus the orientation of hands and feet in "scan motion" is also fixed to make sure they go straight along x-axis. During this motion, distance data measured will be keeping collected. When the "valley" of distance data appears, it means that valid distance data decrease first and then turns to increase, and it is also the indicator that target rung is scanned and passed over by both 2 proximity sensors on an end-effector of WAREC-1.

The process of scan motion can be seen in Fig. 5. l_l and l_r are the distances to target rung measured by proximity sensor on the left and right that are equipped at the same end-effector, respectively. Similarly, x_l and x_r are the distances that the end-effector moves forward in the scan motion (which can be obtained by forward kinematics of the robot) when the sensor on the left and right go over the target rung, respectively. With these 4 variables known, not only the relative distance but also the orientation of target rung can be estimated based on geometric calculations. Detailed algorithms of the whole sensing are presented in Ref. [28] and are omitted.

3.3 Reaction force adjustment in 2-point contact ladder climbing

Besides rung recognition, this subsection discusses reaction force adjustment, a method guaranteeing appropriate reaction force distribution between 2 contact points in ladder climbing for 2-point contact ladder climbing. The authors have proposed a simple control method of reaction force between the robot and ladder for stabilization and verified in simulation[24]. In this paper, new scheme of reaction force control is utilized for 2-point contact ladder climbing of WAREC-1, with details shown below.

It has been explained and verified by the former studies[3,4,10] that bias of reaction force at contact points in ladder climbing may lead to slide due to insufficient friction force at contact point(s) and failure of ladder climbing. Therefore, appropriate distribution of reaction force between 2 contact points that keeps friction cone constraint is crucial to stable ladder climbing in 2-point contact, which can be expressed as:

$$\left\|\boldsymbol{F}^{\mathrm{t}}_{\mathrm{hand}}\right\|_2 \le \mu(\boldsymbol{F}_{\mathrm{hand}} \cdot \boldsymbol{n}_{\mathrm{hand}}), \tag{9}$$

$$\left\|\boldsymbol{F}^{\mathrm{t}}_{\mathrm{foot}}\right\|_2 \le \mu(\boldsymbol{F}_{\mathrm{foot}} \cdot \boldsymbol{n}_{\mathrm{foot}}) \tag{10}$$

where $\boldsymbol{F}_{\mathrm{hand}} = (F_{\mathrm{handx}}, F_{\mathrm{handy}}, F_{\mathrm{handz}})^{\mathrm{T}}$ and $\boldsymbol{F}_{\mathrm{foot}} = (F_{\mathrm{footx}}, F_{\mathrm{footy}}, F_{\mathrm{footz}})^{\mathrm{T}}$ are reaction force on supporting hand and foot, respectively. $\boldsymbol{F}^{\mathrm{t}}_{\mathrm{hand}}$ and $\boldsymbol{F}^{\mathrm{t}}_{\mathrm{foot}}$ are tangential components of $\boldsymbol{F}_{\mathrm{hand}}$ and $\boldsymbol{F}_{\mathrm{foot}}$, respectively. $\boldsymbol{n}_{\mathrm{hand}}$ and $\boldsymbol{n}_{\mathrm{foot}}$ are unit normal vectors at contact point of hand and foot, respectively. μ is the friction coefficient between end-effectors and ladder rungs. Note that in this paper we assume that (i) the friction coefficient μ for hand and foot is identical; (ii) $\boldsymbol{n}_{\mathrm{hand}}$ and $\boldsymbol{n}_{\mathrm{foot}}$ are unit vectors alone z-axis. We have

$$F_{\mathrm{handz}} + F_{\mathrm{footz}} = \sum_i m_i g + \sum_i m_i a_{\mathrm{giz}}, \tag{11}$$

where m_i is the mass of the i_{th} link and a_{giz} is the acceleration of the i_{th} link in Z-axis. From Eq. (11) we see that the sum of reaction force in Z-axis for supporting hand and foot is calculable and the increase of either one directly leads to the decrease of the other. Combining assumptions (i) and (ii) described above and Eq. (11), it can be concluded that

$$F_{\mathrm{handz}} = F_{\mathrm{footz}}, \tag{12}$$

is optimal reaction force distribution in z-axis. In the real application, it is desirable to satisfy the following condition:

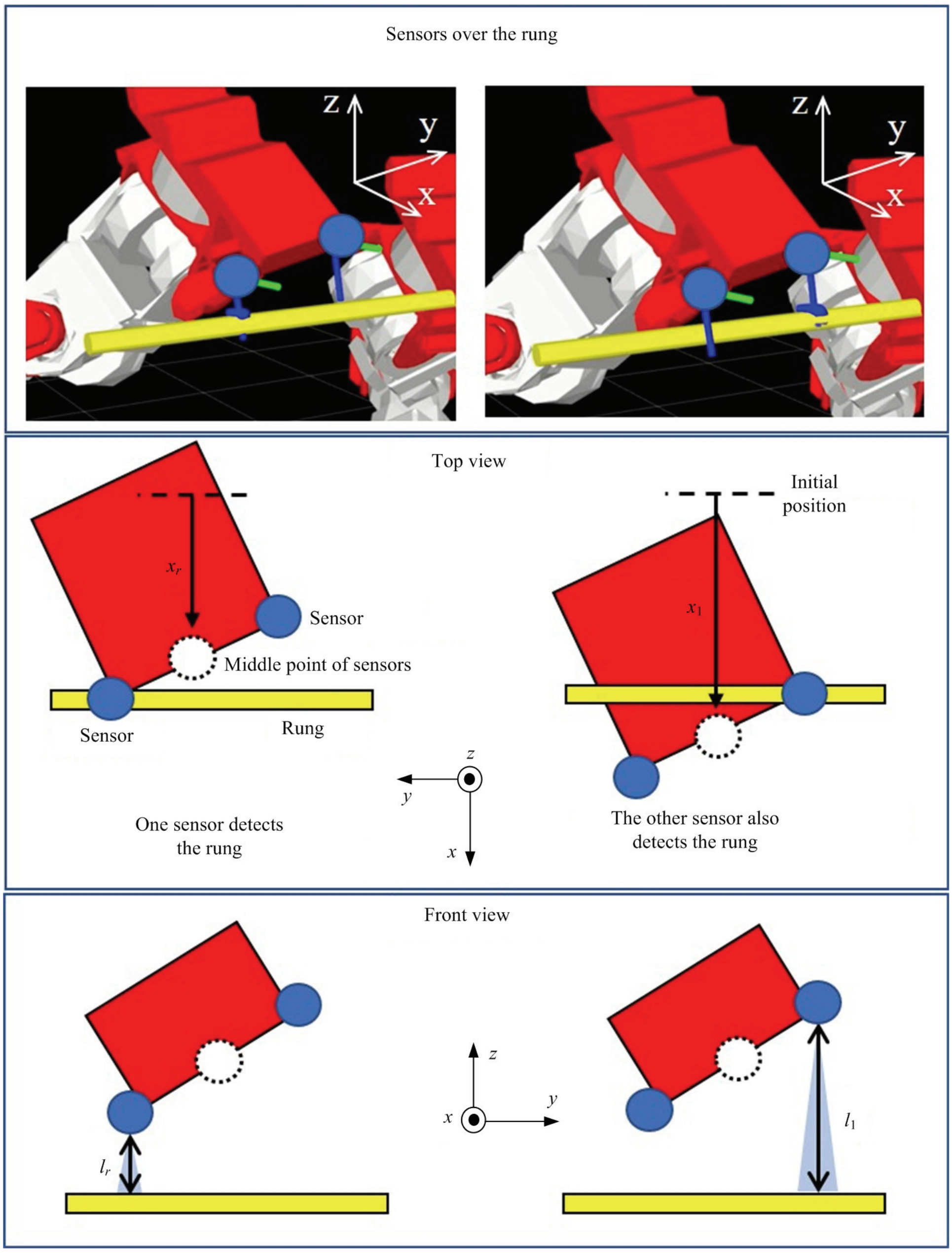

Fig. 5 The sensing process of rung recognition.

$$\left|F_{\text{footz}} - F_{\text{handz}}\right| \le F_{\text{tol}}, \tag{13}$$

where F_{tol} is the tolerance of the difference of 2 forces that satisfies friction cone constraint Eq. (9) and Eq. (10), and its biggest available value is determined by μ (calculations omitted here). If the reaction force in Z-axis on supporting hand/foot is not sufficient to satisfy Eq. (13), then reaction force adjustment for the corresponding hand/foot along z-axis acts until F_{handz} and F_{footz} get close enough to satisfy Eq. (13).

Specifically, we choose PID controller of reaction force with respect to end-effector position in z-axis to control the force at contact point of hand or foot (only for the one with insufficient reaction force). The equation of PID controller is as:

$$\Delta r_z = K_p(F_z - F_{zd}) + K_i\int(F_z - F_{zd})\mathrm{d}t + K_d\frac{\mathrm{d}(F_z - F_{zd})}{\mathrm{d}t}, \tag{14}$$

where Δr_z is the modification amount of position in Z-axis required for the corresponding end-effector, K_p is the proportional gain, K_i is the integral gain, K_d is the derivative gain, F_z is the current value of reaction force in Z-axis, and F_{zd} is the desired value of reaction force in Z-axis.

Finally, the flowchart of motion generation for ladder climbing of WAREC-1 is depicted in Fig. 6.

4 Experiments for evaluation

With all main components introduced, this section presents the evaluation experiments of their integration for both 3-point and 2-point contact ladder climbing gait. In this paper, the target ladder is JIS (Japanese Industrial Standards)-compliant ones, with rung interval within the range of 225 mm ~ 300 mm and rung length (distance between 2 side poles) within the range of 400 mm ~ 600 mm.

In order to evaluate the rung recognition system, not only regular ladders but also 2 irregular cases that may occur are mainly discussed: (i) Ladder with different rung interval, which can usually be seen in low-cost handmade or temporary ladders; (ii) Inclination of rung, which may happen for damaged or aged ladders. To simulate these 2 cases, we made 2 wooden plates and call them "Ladder Attachment 1" and "Ladder Attachment 2" with scales presented in Fig. 7. The change of specification after equipping them is listed in Table 1. The rung interval and rung length of the original ladder in Fig. 7 are 250 mm and 600 mm, respectively.

According to the range of 225 mm ~ 300 mm for rung interval in JIS, the difference between the longest and shortest rung interval is 75 mm. From our view, it means that the error of rung interval is within the range of ±37.5 mm, which is exactly the reason why the change of position in Z-axis for Ladder Attachment 1 is set to 37.5 mm. Due to physical limit, the case of a lower rung is not included.

The reason of 5.0° in inclination angle for Ladder Attachment 2 is based on the range of 400 mm ~ 600 mm for rung length in JIS. For the case with biggest inclination expected, which is the shortest rung length of 400 mm and biggest rung interval error of +37.5 mm, the

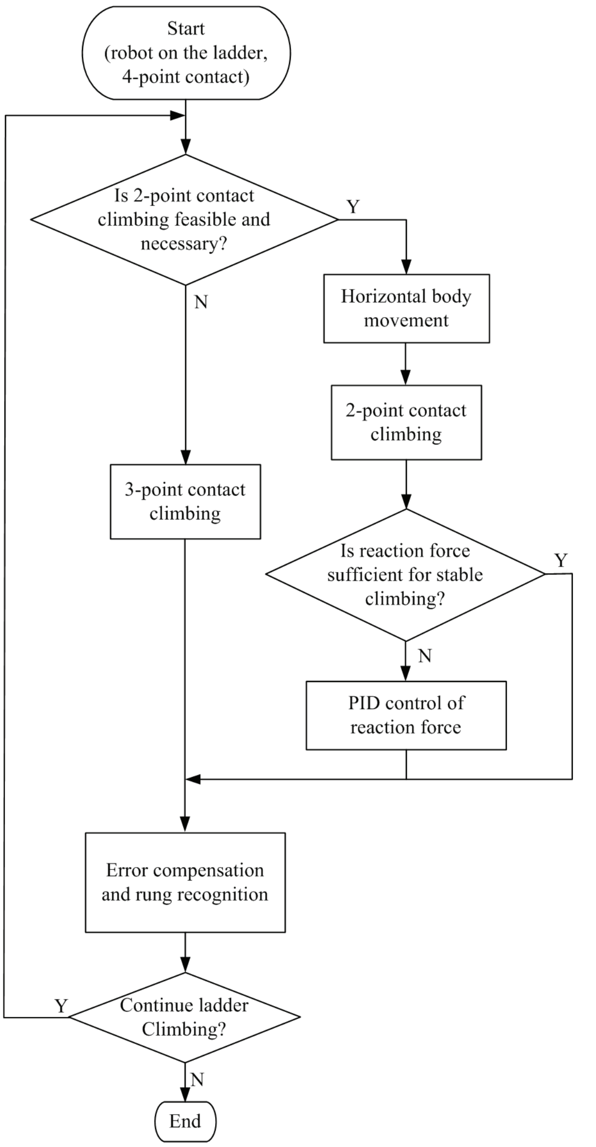

Fig. 6 Flowchart of motion generation for WAREC-1.

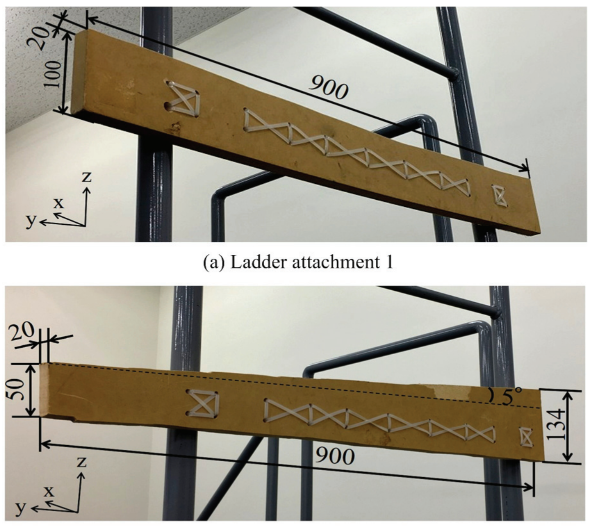

(a) Ladder attachment 1

(b) Ladder attachment 2

Fig. 7 Ladder attachment 1 and 2 with scales.

Table 1 Change of specification

	Ladder attachment 1	Ladder attachment 2
Position in *X*-axis (mm)	−23	−23
Position in *Z*-axis (may slightly change in ladder climbing) (mm)	+37.5	+64 (right) +48 (left)
Inclination angle (˚)	0	5.0 (Roll)

Table 2 Time data

	Ladder attachment 1	Ladder attachment 2
Climbing motion (s)	40 (10 for each limb)	40 (10 for each limb)
Scan and adjustment motion (s)	36 (9 for each limb)	36 (9 for each limb)
Idling (confirming the results and input of commands for safety) (s)	17	9
Total (s)	93	85

inclination angle of the rung in this case is calculated to be about 5.0˚.

4.1 Case 1: 3-point contact ladder climbing

The snapshots of ladder climbing in 3-point contact gait with Ladder Attachment 1 and 2 are shown in Fig. 8 with details of time spent listed in Table 2. The results verify that ladder climbing with rung recognition for Ladder Attachment 1 and 2 is successful. Data of proximity sensors acquired in rung cognition for the experiment with Ladder Attachment 2 are also presented in Fig. 9 as the verification of recognition for rung inclination. From the data in Fig. 9 and forward kinematics of WAREC-1, l_l, l_r, x_l and x_r in Fig. 5 can be obtained. With these 4 variables inclination angles are estimated to be 5.0˚ and 4.2˚ for the left and right hand, respectively, which are both close enough to the real value of 5.0˚.

4.2 Case 2: 2-point contact ladder climbing

Besides the experiments of Case 1 in 3-point contact gait, we also apply the integration of all contents introduced in this paper to 2-point contact ladder climbing for the cases that 3-point contact ladder climbing is too slow to meet the requirements.

The snapshots of 2-point contact ladder climbing with both rung recognition and reaction force adjustment are shown in Fig. 10. Detailed conditions can be seen in Table 3. It only took 20 s to climb up a rung, which is 3.8 times in speed of Case 1. Meanwhile, the reaction force data in *Z*-axis and proximity sensor data of the right

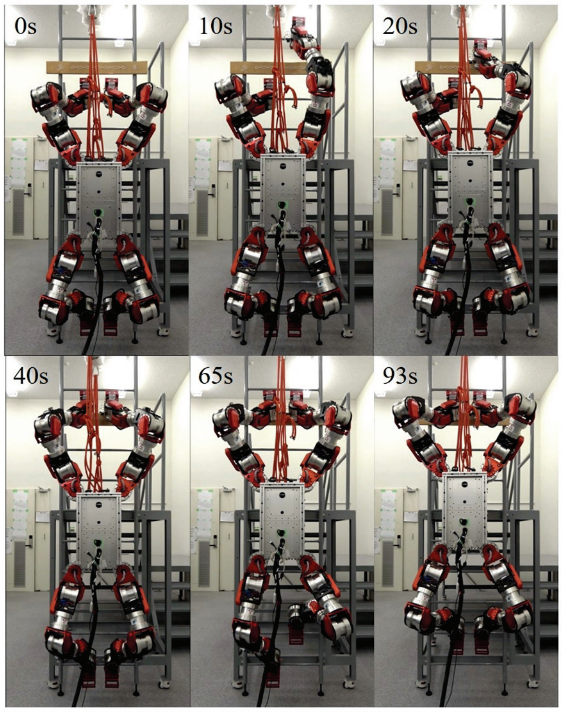

(a) Ladder attachment 1

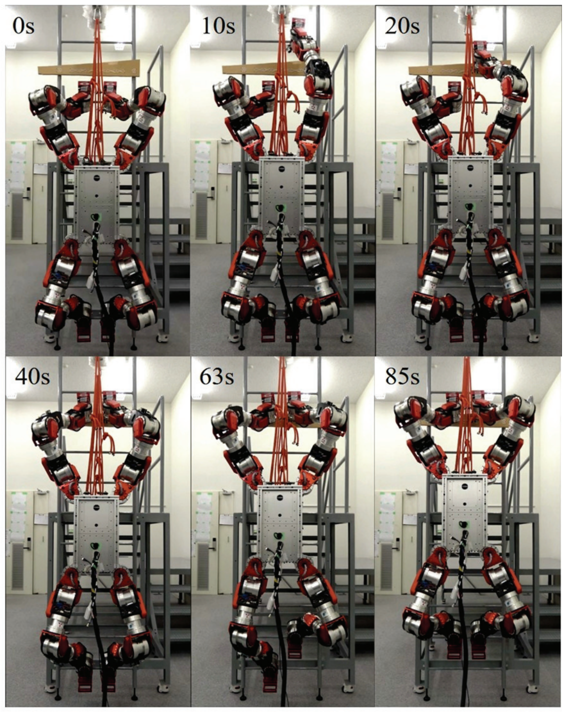

(b) Ladder attachment 2

Fig. 8 Snapshots of ladder climbing for Case 1.

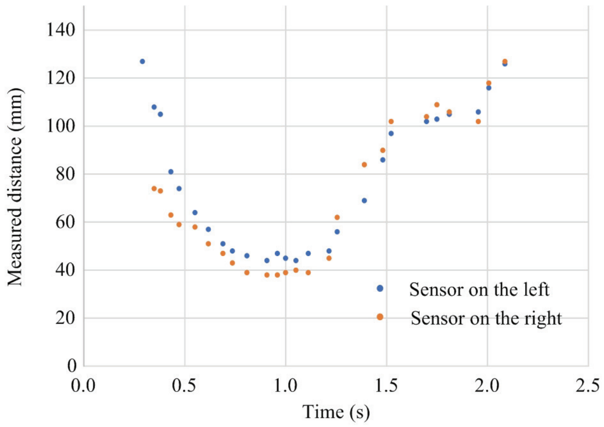

(a) Right hand

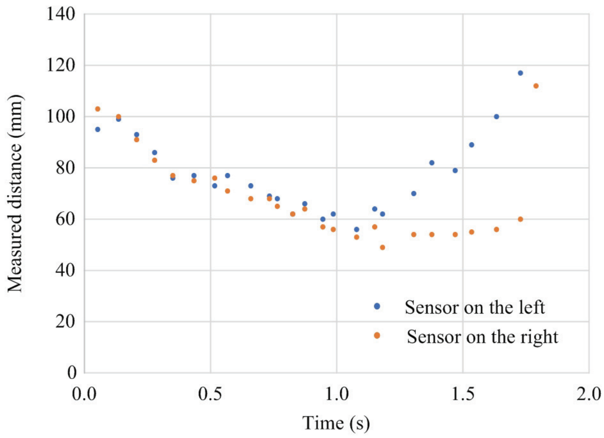

(b) Left hand

Fig. 9 Proximity sensor data of both 2 hands for the case in Fig.8b.

hand are illustrated in Fig. 11 and Fig. 12, respectively. In this case, the biggest value available for F_{tol} in Eq. (13) is calculated to be about 800 N, and in the experiment we set it to be 200 N. Fig. 11 shows that the biggest difference of reaction force in Z-axis at 2 contact points is limited under 200 N, validating that the reaction force adjustment for maintaining the condition Eq. (13) is effective.

As for rung recognition, inclination angle of Ladder Attachment 2 can be estimated in the same way of Case1, which is exactly the real value of 5.0˚.

4.3 Discussion

The results of Case 1 and Case 2 show that climbing a ladder with a different rung interval (37.5 mm higher) or rung inclination (5.0˚) within a certain range by a real human-sized robot in both 3-point contact and 2-point contact gait (about 4 times in speed of 3-point

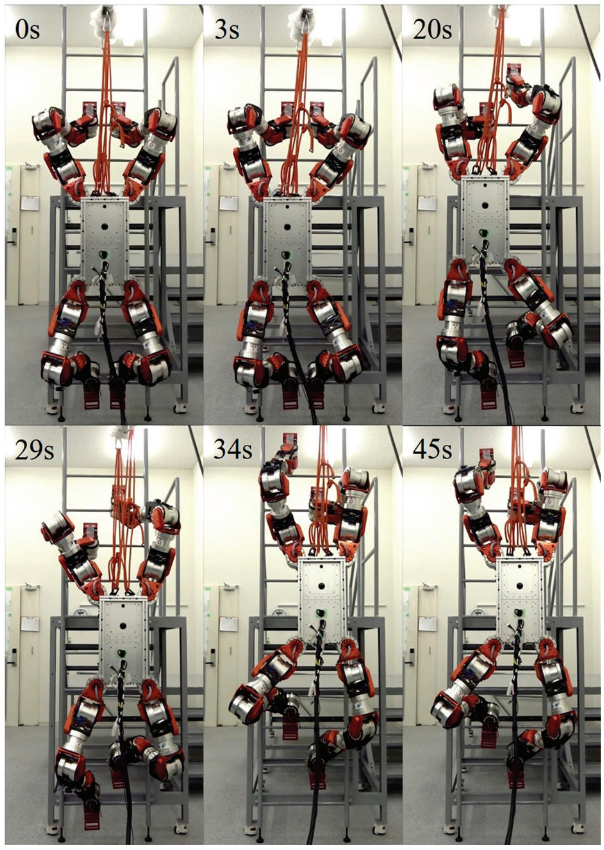

Fig. 10 Snapshots of 2-point contact ladder climbing with rung recognition and reaction force adjustment.

Table 3 Conditions of the total integration experiment

Term	Value/Description
Target rung	Ladder attachment 2
Distance of horizontal body move (mm)	100 (first step) 200 (second step)
Time for 1 climb motion (s)	5
Time for 1 scan motion and compensation motion (s)	12
Time for horizontal body move (s)	2 (first step) 4 (second step)
Time for idling (inputting command) (s)	6
Total time (s)	46
T_{tol} (N)	200

contact gait) is verified to be available with the stabilization system proposed in this paper, which has scarcely been achieved by any existing studies. This indicates huge improvement of robustness for ladder specification in ladder climbing of a human-sized robot. Data of

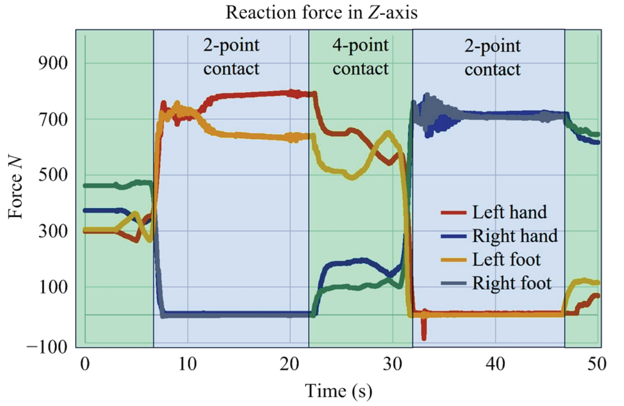

Fig. 11 Reaction force in Z-axis in 2-point contact ladder climbing.

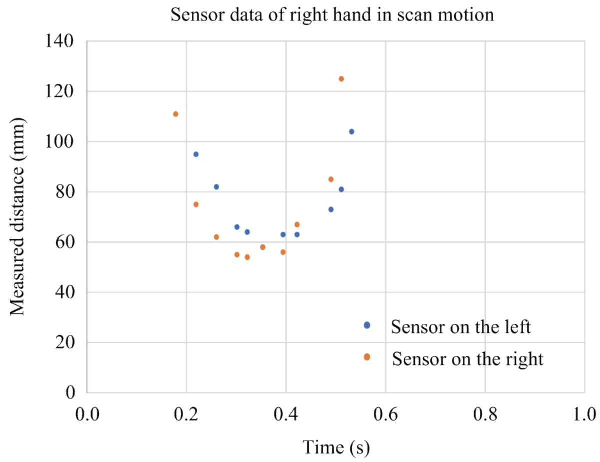

Fig. 12 Proximity sensor data of right hand.

proximity sensors and force/torque sensors also validates the effectiveness of both rung recognition and reaction force adjustment, with slight sensing error in an acceptable range.

However, rung recognition has its limitations and can be further improved in terms of sensing range. At present rung recognition only works with a part of the target rung, which is still far from the whole ladder, which may be insufficient for ladder climbing in more complicated conditions.

5 Conclusion

In this paper, a system maintaining stable ladder climbing of the robot "WAREC-1" with the capability of rung recognition as well as reaction force adjustment for 2-point contact state is described and evaluated in detail. Stability condition of a four-limbed robot on a ladder is proposed, which is the expansion and the improved version of the known one proposed by a former study. Based on that stability condition, 3 components of (i) Whole-body motion planning; (ii) Rung recognition and (iii) Reaction force adjustment are constructed and integrated so that the followings that have hardly been achieved by the former studies become possible: (i) Ladder climbing in 2-point contact gait by a human-sized four-limbed robot, which is much faster than conventional 3-point contact gait but also requires appropriate control of motion and force/torque at contact points; (ii) Climbing of an irregular ladder with a higher/inclined rung in both 3-point and 2-point contact gait by the same robot, which also requires the recognition of ladder rungs and corresponding motion adjustment. The contributions above are expected to improve the capability to climb ladders with unknown or irregular specifications for WAREC-1 and hopefully other human-sized robots. The future work of this study will mainly focus on the realization of global recognition of the whole ladder and its corresponding motion planning system.

Acknowledgment

This research was funded by ImPACT TRC Program of Council for Science, Technology and Innovation (Cabinet Office, Government of Japan). This study was conducted with the support of Research Institute for Science and Engineering, Waseda University; Future Robotics Organization, Waseda University, and as a part of the humanoid project at the Humanoid Robotics Institute, Waseda University. This research was also partially supported by SolidWorks Japan K. K; DYDEN Corporation; and KITO Corporation whom we thank for their financial and technical support.

References

[1] Hashimoto K, Kimura S, Sakai N, Hamamoto S, Koizumi A, Sun X, Matsuzawa T, Teramachi T, Yoshida Y, Imai A, Kumagai K, Matsubara T, Yamaguchi K, Ma G, Takanishi A. WAREC-1 – A four-limbed robot having high locomotion ability with versatility in locomotion styles. *Proceedings of the* 2017 *International Symposium on Safety*, *Security and Rescue Robotics*, Shanghai, China, 2017, 172–178.

[2] Sun X. *The Motion Generation of Stable Vertical Ladder*

Climbing Capable of Recognizing Rungs for a Four-limbed Robot, PhD thesis, Waseda University, Tokyo, Japan, 2018.

[3] Iida H, Hozumi H, Nakayama R. Development of ladder climbing robot LCR-1. *Journal of Robotics and Mechatronics*, 1989, **1**, 311–316.

[4] Yoneda H, Sekiyama K, Hasegawa Y, Fukuda T. Vertical ladder climbing motion with posture control for multi-locomotion robot. *Proceedings of the* 2008 *IEEE/RSJ International Conference on Intelligent Robots and Systems*, Nice, France, 2008, 3579–3584.

[5] Lu Z, Aoyama T, Yoneda H, Sekiyama K, Fukuda T, Hasegawa Y. Vertical ladder climbing motion of pace gait with body motion control for a multi-locomotion robot. *Proceedings of the* 2009 *IEEE/SICE International Symposium on System Integration*, Tokyo, Japan, 2009, 48–53.

[6] Lu Z, Sekiyama K, Hasegawa Y, Aoyama T, Yoneda H, Fukuda T. Climbing up motion of the multi-locomotion robot (MLR) on vertical ladder with different gaits. *International Journal of Mechatronics and Automation*, 2011, **1**, 190–200.

[7] Lu Z, Sekiyama K, Aoyama T, Hasegawa Y, Kobayashi T, Fukuda T. Optimal control of energetically efficient ladder decent motion with internal stress adjustment using key joint method. *Proceedings of the* 2012 *IEEE/RSJ International Conference on Intelligent Robots and Systems*, Vilamoura, Portugal, 2012, 2216–2221.

[8] Feng S, Whitman E, Xinjilefu X, Atkeson C G. Optimization based full body control for the atlas robot. *Proceedings of* 2014 *IEEE-RAS International Conference on Humanoid Robots*, Madrid, Spain, 2014, 120–127.

[9] Vaillant J, Kheddar A, Audren H, Keith F, Brossette S, Kaneko K, Morisawa M, Yoshida E, Kanehiro F. Vertical ladder climbing by HRP-2 humanoid robot. *Proceedings of* 2014 *IEEE-RAS International Conference on Humanoid Robots*, Madrid, Spain, 2014, 671–676.

[10] Vaillant J, Kheddar A, Audren H, Keith F, Brossette S, Escande A, Bouyarmane K, Kaneko K, Morisawa M, Gergondet P, Yoshida E, Kajita S, Kenehiro F. Multi-contact vertical ladder climbing with an HRP-2 humanoid. *Autonomous Robots*, 2016, **40**, 3, 561–580.

[11] Yoshiike T, Kuroda M, Ujino R, Kaneko H, Higuchi H, Iwasaki S, Kanemoto Y, Asatani M, Koshiishi T. Development of experimental legged robot for inspection and disaster response in plants. *Proceedings of the* 2017 *IEEE/RSJ International Conference on Intelligent Robots and Systems*, Vancouver, Canada, 2017, 4869–4876.

[12] Yoshiike T, Kuroda M, Ujino R, Kanemoto Y, Kaneko H, Higuchi H, Komuro S, Iwasaki S, Asatani M, Koshiishi T. The experimental humanoid robot E2-DR: A design for inspection and disaster response in industrial environments. *IEEE Robotics* & *Automation Magazine*, 2019, **26**, 4, 46–58.

[13] Fujii S, Inoue K, Takubo T, Mae Y, Arai T. Ladder climbing control for limb mechanism robot "ASTERISK". *Proceedings of the* 2008 *IEEE International Conference on Robotics and Automation*, Pasadena, USA, 2008, 3052–3057.

[14] Saputra A A, Toda Y, Takesue N, Kubota N. A novel capabilities of quadruped robot moving through vertical ladder without handrail support. *Proceedings of the* 2019 *IEEE/RSJ International Conference on Intelligent Robots and Systems*, Macau, China, 2019, 1448–1453.

[15] Moey L K, Teng N L S, Ng J Y, Solihin M I, Badrulhisam N H. Design and development of ladder climbing robot. *Applied Mechanics and Materials*, 2020, **899**, 31–41.

[16] Takemori T, Tanaka M, Matsuno F. Gait design for a snake robot to climb a ladder. *Proceedings of the* 2017 *International Symposium on Swarm Behavior and Bio-Inspired Robotics*, Kyoto, Japan, 2017, 89–92.

[17] Takemori T, Tanaka M, Matsuno F. Ladder Climbing with a Snake Robot. *Proceedings of the* 2018 *IEEE/RSJ International Conference on Intelligent Robots and Systems*, Madrid, Spain, 2018, 1–9.

[18] Zhang Y, Luo J, Hauser K, Ellenberg B, Oh P, Park H A, Paldhe M, Lee C S G. Motion planning of ladder climbing for humanoid robots, *Proceedings of the* 2013 *International Conference on Technologies for Practical Robot Applications*, Woburn, USA, 2013, 1–6.

[19] Luo J, Zhang Y, Hauser K, Park H A, Paldhe M, Lee C S G, Grey M, Stilman M, Oh J H, Lee J, Kim I, Oh P. Robust ladder-climbing with a humanoid robot with application to the DARPA robotics challenge. *Proceedings of the* 2014 *IEEE International Conference on Robotics and Automation*, Hong Kong, China, 2014, 2792–2798.

[20] Kanazawa M, Nozawa S, Kakiuchi Y, Kanemoto Y, Kuroda M, Okada K, Inaba M, Yoshiike T. Robust vertical ladder climbing and transitioning between ladder and catwalk for humanoid robots. *Proceedings of the* 2015 *IEEE/RSJ International Conference on Intelligent Robots and Systems*, Hamburg, Germany, 2015, 2202–2009.

[21] Nozawa S, Kanazawa M, Kakiuchi Y, Okada K, Yoshiike T, Inaba M. Three-dimensional humanoid motion planning using COM feasible region and its application to ladder climbing tasks. *Proceedings of the* 2016 *IEEE-RAS* 16*th International Conference on Humanoid Robots*, Cancun, Mexico, 2016, 49–56.

[22] Gyawali P, McGough J. Simulation of detecting and climbing a ladder for a humanoid robot. *Proceedings of the* 2013 *IEEE International Conference on Electro-Information Technology*, Rapid City, USA, 2013, 1–6.

[23] Sun X, Hashimoto K, Hamamoto S, Koizumi A, Matsuzawa T, Teramachi T, Takanishi A. Trajectory generation for ladder climbing motion with separated path and time planning. *Proceedings of the* 2016 *IEEE/RSJ International Conference on Intelligent Robots and Systems*, Daejeon, Korea, 2016, 5782–5788.

[24] Sun X, Hashimoto K, Teramachi T, Matsuzawa T, Kimura S, Sakai N, Hayashi S, Yoshida Y, Takanishi A. Planning and control of stable ladder climbing motion for the four-limbed robot “WAREC-1”. *Proceedings of the* 2017 *IEEE/RSJ International Conference on Intelligent Robots and Systems*, Vancouver, Canada, 2017, 6547–6554.

[25] Matsuzawa T, Hashimoto K, Sun X, Teramachi T, Kimura S, Sakai N, Yoshida Y, Imai A, Kumagai K, Matsubara T, Yamaguchi K, Tan W, Takanishi A. Crawling gait generation method for four-limbed robot based on normalized energy stability margin. *Proceedings of the* 2017 *International Symposium on Safety*, *Security and Rescue Robotics*, Shanghai, China, 2017, 223–229.

[26] Matsuzawa T, Hashimoto K, Teramachi T, Uryu K, Sun X, Hamamoto S, Koizumi A, Takanishi A. End-effector for disaster response robot with commonly structured limbs and experiment in climbing vertical ladder. *ROMANSY* 21-*Robot Design*, *Dynamics and Control*, 2016, 311–319.

[27] VL6180 Infrared proximity sensor module (in Japanese), [2020-04-23], https://www.switch-science.com/catalog/2518/.

[28] Sun X, Hayashi S, Hashimoto K, Matsuzawa T, Yoshida Y, Sakai N, Imai A, Okawara M, Kumagai K, Matsubara T, Yamaguchi K, Takanishi A. Error Compensation System with Proximity Sensors for Vertical Ladder Climbing of the Robot “WAREC-1”. *Proceedings of the* 2018 *IEEE-RAS International Conference on Humanoid Robots*, Beijing, China, 2018, 40–46.